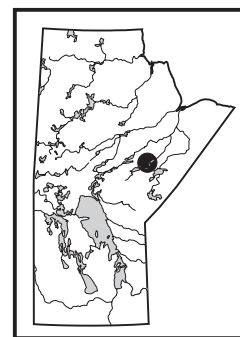


## GS-10 Evaluation of the age, extent and composition of the Cinder Lake alkaline intrusive complex, Knee Lake area, Manitoba (part of NTS 53L15)

by A.R. Chakhmouradian<sup>1</sup>, C.O. Böhm, R.D. Kressall<sup>1</sup> and P.G. Lenton

Chakhmouradian, A.R., Böhm, C.O., Kressall, R.D. and Lenton, P.G. 2008: Evaluation of the age, extent and composition of the Cinder Lake alkaline intrusive complex, Knee Lake area, Manitoba (part of NTS 53L15); in Report of Activities 2008, Manitoba Science, Technology, Energy and Mines, Manitoba Geological Survey, p. 109–120.



### Summary

A detailed reinvestigation of alkaline igneous rocks from the southwestern part of Cinder Lake (Gods Lake Domain) was initiated as a joint project between the Manitoba Geological Survey and Department of Geological Sciences, University of Manitoba. At least three discrete intrusive phases can be identified at present on the basis of field and petrographic evidence (listed in order of emplacement): fine-grained aegirine-nepheline syenite, fine-grained biotite-vishnevitte syenite and syenitic pegmatite. There is also convincing mineralogical and geochemical evidence for the presence of unexposed ultramafic and carbonatitic units genetically associated with the alkaline syenitic rocks. Uranium-lead dating of zircon crystals recovered from a sample of biotite-vishnevitte syenite yielded an age of  $2705 \pm 2$  Ma, which is tentatively being interpreted as the timing of syenite formation and emplacement. The Cinder Lake rocks exhibit a trace-element signature indicative of arc settings, which fits into a subduction-collision tectonic regime for this part of the Gods Lake Domain at ca. 2.7 Ga.

### Introduction

Silica-undersaturated alkaline rocks at Cinder Lake in the northwestern Superior Province in Manitoba were first mapped by Elbers (*in* Gilbert, 1985) and Lenton (1985), and described as a suite of syenitic rocks associated with the Bayly Lake plutonic complex (Gilbert, 1985). The Cinder Lake locality remains the only known occurrence of feldspathoid rocks in Manitoba to date. Intrusive rocks making up the Cinder Lake complex show little evidence of deformation and metamorphism and, as such, present a unique opportunity to gain insight into the evolution of the Archean mantle beneath the Superior plate prior to its collision with the Sask and Hearne plates. The extent of alkaline magmatism at Cinder Lake is uncertain, however, and neither the petrography nor the geochemistry of these rocks has been studied in adequate detail. To address these deficiencies, the authors re-examined material collected by P. Lenton and undertook further fieldwork and sampling in the southeastern part of Cinder Lake in June 2008. This report is a brief summary of observations and findings to date.

### Geological overview of the Cinder Lake area

The study area is located in the central part of the Neoproterozoic Gods Lake Domain (GLD), the largest greenstone-granite belt in the northwestern Superior Province (Figure GS-10-1). The GLD is a sublatitudinal structure extending from west of Cross Lake across central Manitoba for a distance of ~400 km into northwestern Ontario, where it continues as the Stull Domain within the Archean Sachigo subprovince (e.g., Stott and Rayner, 2004). Cinder Lake is accessible by floatplane or boat from Oxford House, some 27 km to the west, and from the North Star resort at nearby Knee Lake. In the vicinity of Cinder Lake, the GLD comprises three distinct tectono-stratigraphic units, termed the Gods Lake Group, the Bayly Lake complex and the Oxford Lake Group (Gilbert, 1985; Corkery et al., 2000). The Gods Lake Group, also referred to as the Hayes River Group, consists mostly of volcanic rocks dominated by pillow basalt and associated gabbro with subordinate intermediate and felsic volcanic and volcano-sedimentary rocks (Syme et al., 1997; Corkery et al., 2000). The felsic volcanic rocks and synvolcanic greywacke were emplaced around 2.83–2.82 Ga (Corkery et al., 2000; Lin et al., 2006). Immediately west of Cinder Lake and east-southeast of Knee Lake, the rocks of the Gods Lake Group are intruded by granitic plutons collectively referred to as the Bayly Lake complex (Gilbert, 1985). This complex comprises a wide spectrum of granitic rocks emplaced in a variety of tectonic settings between 2.78 and 2.73 Ga (Corkery et al., 2000). The Oxford Lake Group is a thick package of clastic sedimentary rocks (ranging from polymictic conglomerate to greywacke) deposited in a subaerial or shallow-marine environment around 2.71 Ga (Corkery et al., 2000). The clastic sedimentary rocks are underlain by a discontinuous unit of shoshonitic to calcalkaline volcanic rocks and associated siltstone and sandstone dated at ca. 2.72 Ga (Gods Lake Narrows Group of Lin et al., 2006). West and southwest of Cinder Lake, the volcanic rocks of the Gods Lake Group are separated from the Oxford Lake Group by an east-southeast-trending shear zone with transpressional kinematics (Lin and Jiang, 2001). In this part of the GLD, the supracrustal rocks are metamorphosed under greenschist- to amphibolite-facies conditions and

<sup>1</sup> Department of Geological Sciences, University of Manitoba, 125 Dysart Road, Winnipeg, Manitoba R3T 2N2

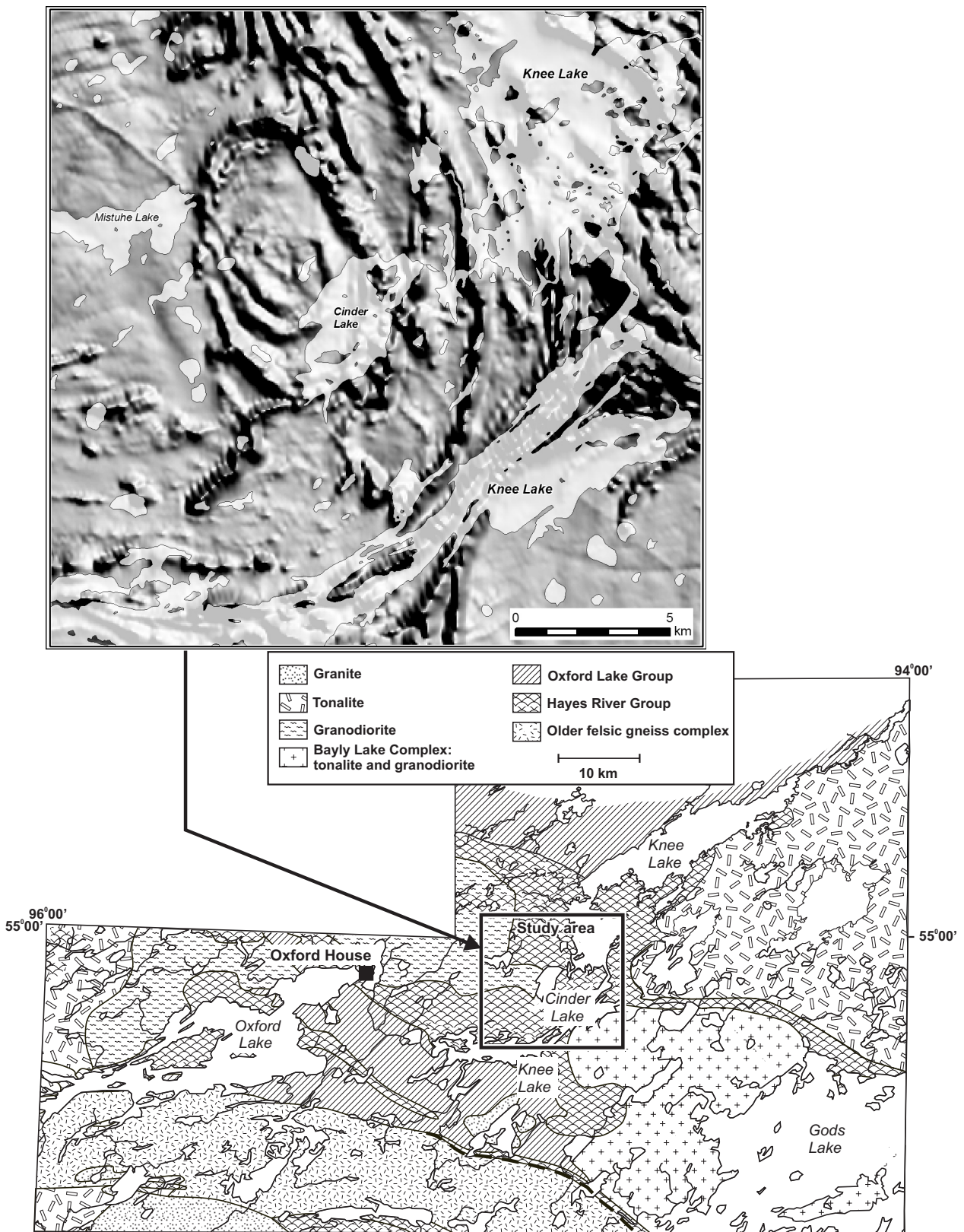


**Figure GS-10-1:** Simplified geology of the Knee Lake area. Insert shows greyscale magnetic residual total field map of the Cinder Lake area.

deformed to various degrees depending on the rock type and proximity to shear zones (Lin et al., 2006). The supracrustal Oxford-Stull Terrane, incorporating the GLD, has been interpreted as a Neoproterozoic collision zone between the North Caribou and North Superior microcontinents (Corkery et al., 1992; Percival et al., 2006).

In the southeastern part of Cinder Lake, the volcanic rocks of the Gods Lake Group host a suite of alkaline igneous rocks showing a wide range of textures and modal compositions. Because of scarce outcrop, the extent of the alkaline igneous complex, particularly in the western and northwestern parts of the lake, is poorly constrained. High-resolution aeromagnetic data of the area, however, outline the possible shape and size of the Cinder Lake intrusive complex (Figure GS-10-1). In the southeastern part of the lake, linear magnetic highs coincide with exposures of syenitic pegmatite (see below) that appear to occupy the outer shell of a concentrically structured intrusive body.

At present, three distinct intrusive units can be readily identified at both outcrop and microscopic scales: 1) fine-grained aegirine-nepheline syenite (unit 1); 2) fine-grained biotite-vishneville syenite (unit 2); and 3) coarse-grained syenitic pegmatite (unit 3). The exposure of unit 1 is limited to the shoreline of several small islands in the southeastern part of Cinder Lake (Figure GS-10-2a), whereas unit 2 appears to be confined to a series of small, largely submerged outcrops along the southeastern shore of the lake. Unit 2 is crosscut by numerous veins of coarse-grained black andradite ranging from a few millimetres to several centimetres in width (Figure GS-10-2b). Structural relations between units 1 and 2 and their country rocks could not be observed because of poor exposure. The syenitic pegmatite is the best exposed unit, forming a 500 m long ridge northeast of, and adjacent to, unit 2 (Figure GS-10-2c). The eastern contact between the pegmatite and surrounding volcanic rocks is marked by a change from predominantly deciduous (alder, birch

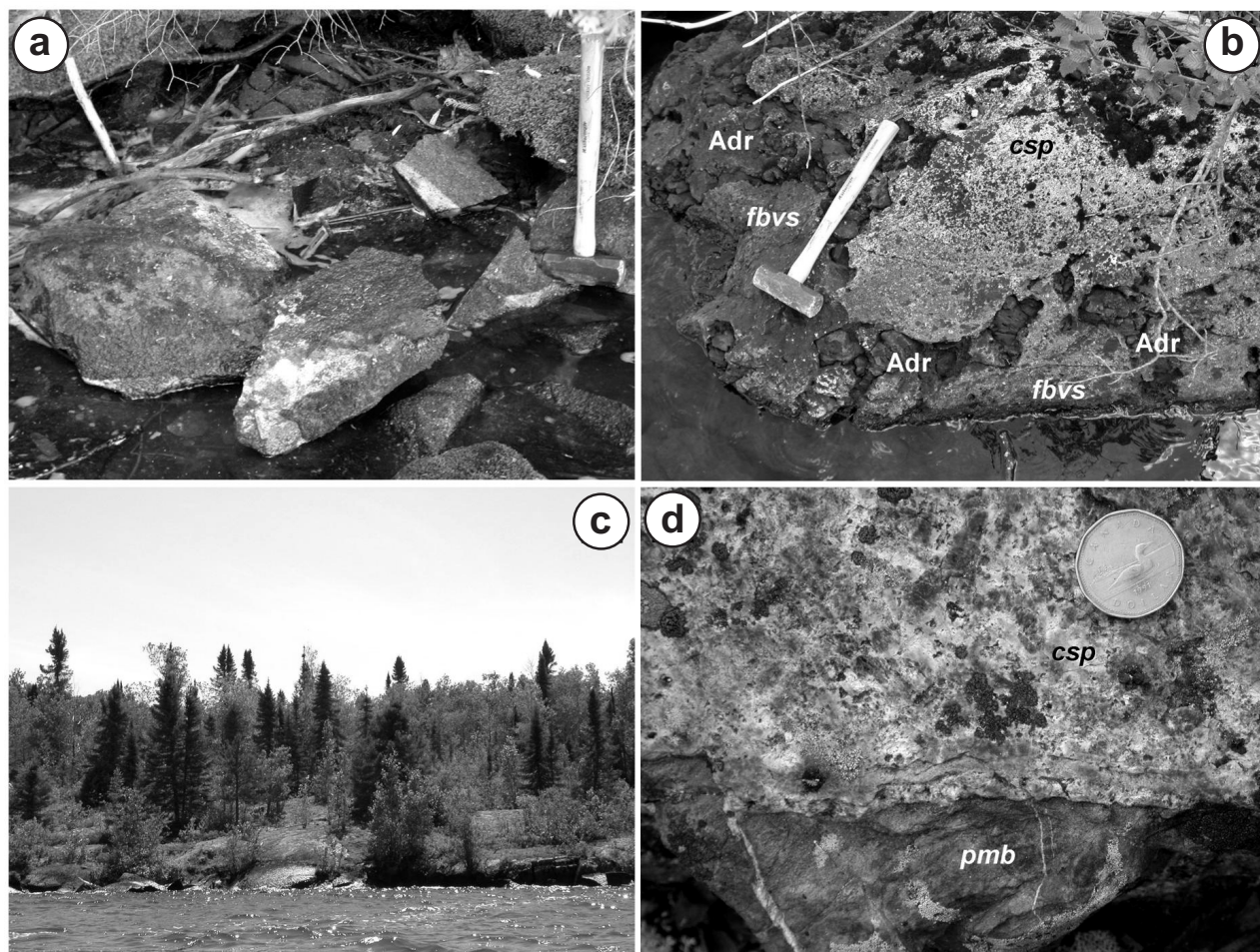


**Figure GS-10-2:** Three major types of alkaline intrusive rocks exposed in the southeastern part of Cinder Lake: **a)** fine-grained aegirine-nepheline syenite (unit 1), forming a limited exposure and rubble pile on a small island in the eastern part of the lake; **b)** fine-grained biotite-vishneville syenite (fbvs, unit 2), containing a segregation of coarse-grained syenitic pegmatite (csp, unit 3) and crosscut by veins of coarse-grained andradite (Adr); **c)** northern face of a ridge made up largely of syenitic pegmatite (unit 3); and **d)** dike of syenitic pegmatite (csp, unit 3), crosscutting plagioclase-phyric massive basalt (pmb).

and poplar) vegetation, supported by the pegmatite, to coniferous vegetation, supported by the country rocks. Isolated pegmatite bodies are also found as small segregations in unit 2 and as dikes up to 3 m thick crosscutting basalt and gabbro along the southern shore of the lake (Figure GS-10-2b, -2d). A conservative estimate of the total area occupied by the alkaline rocks at the current level of erosion is 3–5 km<sup>2</sup>.

### U-Pb zircon age of a syenite sample from Cinder Lake

In order to constrain the timing of magmatism and emplacement of the Cinder Lake alkaline intrusive complex and integrate it into the tectonic evolution of the Knee Lake area, a portion of syenite sample 37-84-142-1A, collected by P. Lenton in 1984 on an island in south-central Cinder Lake, was selected for U-Pb zircon dating. The sample is from a fine-grained mesocratic syenite that contains biotite and vishnevite (unit 2).

#### Methodology

Approximately 2 kg of homogeneous and representative material from sample 37-84-142-1A were processed at the University of Alberta Radiogenic Isotope Facility in Edmonton, Alberta, for mineral separation and U-Pb isotopic analysis for zircon geochronology. The sample yielded a moderate amount of pink zircon fragments.

A selection of hand-picked, representative and best quality zircon fragments was used for conventional U-Pb dating by isotope dilution–thermal ionization mass spectrometry (ID-TIMS), generally following the procedures outlined in Heaman et al. (2002). All analyses were performed on a VG354 mass spectrometer operated

in single Faraday or Daly (analogue) collector peak-hopping mode, and were corrected for mass discrimination based on replicate measurement of the NBS981 and U500 standards. In addition, all measurements obtained with the Daly photomultiplier detector were adjusted for detector bias. The isotopic composition of common Pb in excess of analytical blank (2 pg of Pb) was calculated using the two-stage model of Stacey and Kramers (1975). The resulting U-Pb isotopic zircon data are listed in Table GS-10-1 and plotted as a concordia diagram in Figure GS-10-3. All errors reported in Table GS-10-1 are quoted at 1σ and were calculated by numerical propagation of all known sources of uncertainty. The concordia diagram in Figure GS-10-3 was generated using the Isoplot version 3.0 application of Ludwig (2003), and the error ellipses on the diagram are shown at 2σ.

A total of five zircon analyses, each incorporating between 6 and 20 fragments of similar size and shape, yielded variably discordant U-Pb ages (Table GS-10-1, Figure GS-10-3). The range in U and Th concentrations is moderate, suggesting that the analyzed zircon fractions may be cogenetic. A Th/U value of 0.45–0.87 and partially preserved euhedral morphology are both indicative of igneous zircon. For all five analyses, the calculated <sup>207</sup>Pb/<sup>206</sup>Pb (minimum) ages range between 2667 and ca. 2730 Ma, the latter being reversely discordant and having a large error (analysis 2z in Table GS-10-1). Best-fit regression without analysis 2z results in concordia intercepts at 154 ± 110 Ma and 2702 ± 10 Ma (Figure GS-10-3). The three least discordant and most precise analyses (z3 to z5; Table GS-10-1) give a narrow range of <sup>207</sup>Pb/<sup>206</sup>Pb ages between 2699 and 2695 Ma, which can thus be interpreted as an estimate for the minimum age of zircon

**Table GS-10-1: U-Pb isotope dilution–thermal ionization mass spectrometry (ID-TIMS) analytical data for igneous zircons from Cinder Lake syenite sample 37-84-142-1A.**

Analysis number	Description of zircon fragments analyzed <sup>a</sup>	Weight (mg)	U (ppm)	Th (ppm)	Pb (ppm)	Th/U	TCPB (pg)
1z	larger pink irreg frags (9)	18.0	288	149	116	0.518	96
2z	small pink irreg frags (20)	20.0	122	107	165	0.873	1913
3z	equant dark pink frags (6)	6.0	167	71	96	0.424	38
4z	light pink irreg frags (17)	10.0	106	54	61	0.514	16
5z	dark pink irreg frags (11)	15.0	150	68	80	0.455	40

Analysis number	Isotopic ratios <sup>b</sup>				Model ages (Ma) <sup>b</sup>			Disc. (%)
	<sup>206</sup> Pb/ <sup>204</sup> Pb	<sup>206</sup> Pb/ <sup>238</sup> U	<sup>207</sup> Pb/ <sup>235</sup> U	<sup>207</sup> Pb/ <sup>206</sup> Pb	<sup>206</sup> Pb/ <sup>238</sup> U	<sup>207</sup> Pb/ <sup>235</sup> U	<sup>207</sup> Pb/ <sup>206</sup> Pb	
1z	1150	0.33224±43	8.3153±113	0.18152±11	1849.3±2	2266.0±1	2666.8±1	35.2
2z	58	0.5495±295	14.2827±1822	0.18851±199	2823.1±12	2768.7±15	2729.2±17	-4.3
3z	863	0.48516±63	12.3791±185	0.18506±15	2549.7±3	2633.6±2	2698.7±1	6.7
4z	2132	0.49086±54	12.49443±1442	0.18461±8	2574.4±2	2642.3±1	2694.7±1	5.4
5z	1576	0.45595±52	11.61451±1374	0.18475±9	2421.6±2	2573.8±1	2696.0±1	12.2

<sup>a</sup> Abbreviations: Disc., discordance; irreg, irregular; frags, fragments; (n), number of fragments

<sup>b</sup> Isotopic ratios and ages are corrected for fractionation, blank, spike and initial common lead (Stacey and Kramers, 1975)

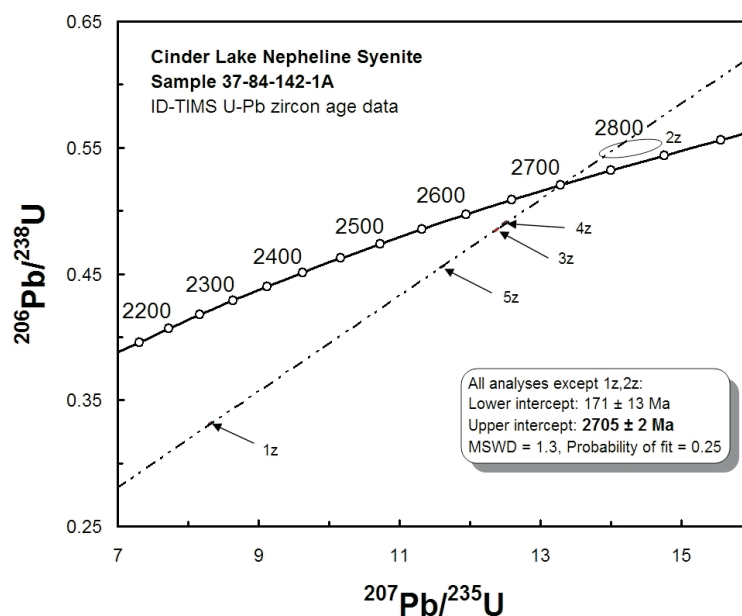


**Figure GS-10-3:** U-Pb concordia diagram for igneous zircons from Cinder Lake syenite sample 37-84-142-1A. A discussion of the preferred interpretation and geological significance of the U-Pb analytical data is provided in the text.

in the biotite-vishnevite syenite. Regression of these three analyses results in a lower intercept at  $171 \pm 13$  Ma and an upper intercept at  $2704.9 \pm 1.9$  Ma on the concordia line (Figure GS-10-3). On the basis of these data, the emplacement age of unit 2 is interpreted to be  $2705 \pm 2$  Ma, assuming that the analyzed zircon fragments are magmatic.

In comparison with granitic plutons of the Bayly Lake complex immediately west of Cinder Lake and east-southeast of Knee Lake, whose ages range between ca. 2.78 and 2.73 Ga (Gilbert, 1985; Corkery et al., 2000), the ca. 2705 Ma age of the syenite indicates that the alkaline intrusive rocks at Cinder Lake are not related to, but are intrusive into, the Bailey Lake granitic suite. On a regional scale, 2.71–2.70 Ga marks incipient accretion of terranes and subprovinces in the northwestern Superior Province (Davis et al., 2005). Consequently, mantle to lower crustal magmatism and formation of the Cinder Lake alkaline intrusive complex may be related to subduction-induced melting between the North Superior and North Caribou superterranes (e.g., Percival et al., 2006).

### Petrography and mineral chemistry

The petrography of the Cinder Lake samples was studied in polished thin sections using polarizing optical microscopy, back-scattered electron (BSE) imaging and energy-dispersive x-ray spectrometry (EDS). The chemical compositions of selected minerals were determined by wavelength-dispersive x-ray spectrometry (WDS) using a fully automated Cameca SX100 electron microprobe

operated at 15 kV and 20 nA. For each mineral or group of minerals, a set of appropriate matrix-specific standards (both natural and synthetic) and optimal instrumental conditions (beam settings, detector type, counting statistics, etc.) were carefully chosen.

The unit 1 rocks, classified as fine-grained aegirine-nepheline syenite, consist of abundant clinopyroxene phenocrysts up to 3 mm across set in a fine-grained allotropic matrix composed of microcline, nepheline, albite and sodalite (listed in order of decreasing abundance). None of the felsic minerals exceeds 0.8 mm in grain size (Figure GS-10-4a). Another prominent textural feature of this rock is the presence of biotite as small (0.1–0.2 mm) crystals associated with nepheline and as large poikilitic plates up to 2.5 mm across (Figure GS-10-4b, -4d). Accessory minerals include apatite, titanite and magnetite (Figure GS-10-4d). Large clinopyroxene phenocrysts comprise Ca-deficient, Al-rich diopside cores rimmed by aegirine (Figure GS-10-4b). This zoning reflects a compositional trend from  $\text{Di}_{59}\text{En}_{16}\text{Hd}_{13}\text{Jd}_7\text{CAT}_5$  in the core to  $\text{Ae}_{47-77}\text{Di}_{18-32}\text{Hd}_{5-28}$  in the rim; the zoning is not continuous, indicating a gap in crystallization. Smaller clinopyroxene crystals lack a Ca-rich core and exhibit a compositional range overlapping that of the aegirine rim of the larger crystals. All aegirine crystals exhibit a reaction rim (Figure GS-10-4c) of low-(Al, Ti) andradite (2.1–4.8 wt. %  $\text{Al}_2\text{O}_3$ ; 0.1–0.7 wt. %  $\text{TiO}_2$ ). Biotite is not zoned and shows little compositional variation (mg #<sup>3</sup> = 0.33–0.36;  $\text{Al}_2\text{O}_3$  = 19.0–19.8 wt. %;  $\text{TiO}_2$  = 0.2–0.5 wt. %; F = 0.2–0.3 wt. %).

<sup>2</sup> Di =  $\text{CaMgSi}_2\text{O}_6$ ; En =  $\text{Mg}_2\text{Si}_2\text{O}_6$ ; Hd =  $\text{CaFeSi}_2\text{O}_6$ ; Jd =  $\text{NaAlSi}_2\text{O}_6$ ; CAT =  $\text{CaAlAlSiO}_6$ ; Ae =  $\text{NaFeSi}_2\text{O}_6$  (all end-member components in mole percent)

<sup>3</sup> mg # =  $\text{Mg}/(\text{Mg}+\text{Fe}_2)$

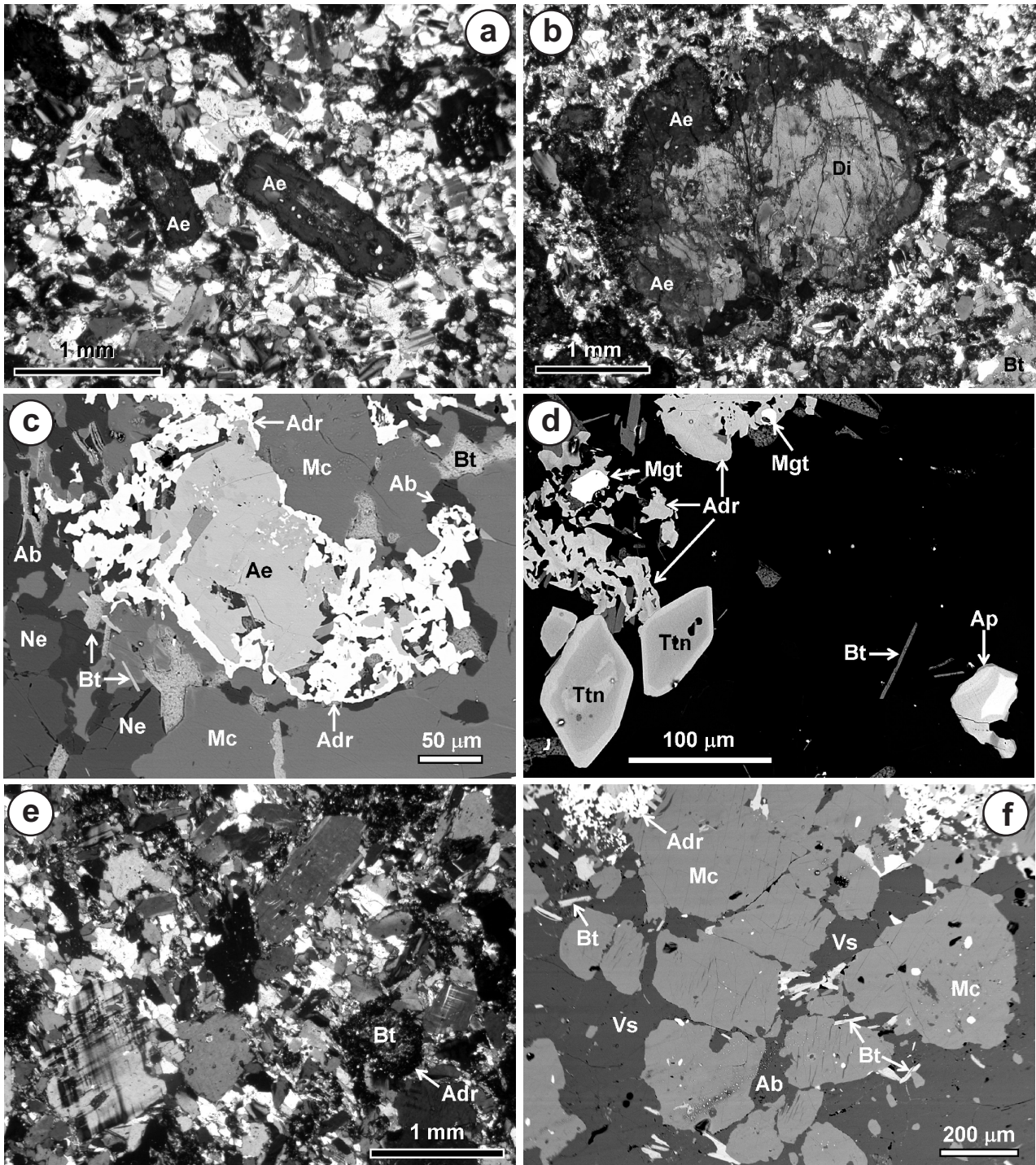


**Figure GS-10-4:** Textural characteristics of feldspathoid syenites from the Cinder Lake alkaline intrusive complex: **a**) aegirine phenocrysts (Ae) in a matrix of microcline, nepheline and albite (unit 1), crossed-polarized light; **b**) aegirine phenocryst (Ae) with a relict diopside core (Di) and poikilitic biotite (Bt) in a felsic matrix (unit 1), crossed-polarized light; **c**) replacement of aegirine (Ae) by andradite (Adr) in unit 1, with associated minerals biotite (Bt), microcline (Mc), nepheline (Ne) and albite (Ab), BSE image; **d**) accessory magnetite (Mgt), titanite (Ttn), apatite (Ap) and andradite (Adr) in unit 1, BSE image; **e**) replacement of biotite (Bt) by andradite (Adr) in unit 2, with felsic groundmass composed of microcline, vishneville and albite, crossed-polarized light; **f**) textural relations between microcline (Mc), vishneville (Vs) and albite (Ab) in unit 2, BSE image.

Microcline, nepheline and albite are also chemically homogeneous and have compositions ( $\text{Kfs}_{95-96}\text{Ab}_{3-4}\text{Cs}_{1-2}$ ,  $\text{Ne}_{74-75}\text{Ks}_{21-22}\text{Qtz}_{3-4}$  and  $\text{Ab}_{99-100}\text{Kfs}_{0-1}$ , respectively) that approach end-member compositions.

The unit 2 rocks, classified as fine-grained biotite-vishnevite syenite, are composed of rare twinned microcline and titanite phenocrysts (up to 7 mm in length), clusters of aegirine crystals and platy biotite set in an allotriomorphic matrix of microcline, vishnevite, albite and sodalite (listed in order of decreasing abundance). The matrix minerals do not exceed, and are generally much less than, 1.5 mm in grain size (Figure GS-10-4e, -4f). Vishnevite is a cancrinite group mineral that has a low birefringence ( $\sim 0.01$ ) and contains appreciable S and Cl; its identification was confirmed by EDS. Accessory constituents are andradite, apatite, allanite, magnetite, pyrite and zircon. Characteristically, aegirine crystals lack diopside cores and are locally replaced by biotite and andradite. Biotite, also pervasively replaced by andradite, is poorer in Al but richer in Mg and Ti in comparison with biotite from unit 1 ( $\text{mg} \# = 0.41\text{--}0.44$ ;  $\text{Al}_2\text{O}_3 = 16.4\text{--}17.2$  wt. %;  $\text{TiO}_2 = 0.5\text{--}0.6$  wt. %;  $\text{F} = 0.2\text{--}0.5$  wt. %). Microcline, albite and andradite are compositionally similar to those in the aegirine-nepheline syenite.

The unit 3 pegmatite (Figure GS-10-5a) comprises dark-brown euhedral crystals of potassium feldspar up to several centimetres in length in a fine-grained pink to green aggregate of muscovite, albite and calcite (listed in order of decreasing abundance). The amounts of potassium feldspar and calcite-albite-muscovite aggregate, as well as the percentage of albite in the aggregate, vary greatly across the pegmatite outcrop. The modal content of albite is the highest where the crystals of potassium feldspar were extensively albitized along their edges and cleavage planes; locally, the primary feldspar is completely pseudomorphed by albite (Figure GS-10-5b, -5c). These highly modified varieties of pegmatite appear to be more susceptible to weathering than fresh pegmatite and may explain variable exposure across the pegmatite body at southeast Cinder Lake, where resistant pegmatite ridges up to several metres wide alternate with zones of no exposure that are subparallel to the magnetic highs in the area (Figure GS-10-1).

The feldspar crystals in the syenitic pegmatite are strongly zoned (Figure GS-10-5d); their cores are enriched in Ba (up to 3.4 wt. % BaO; overall compositional range  $\text{Kfs}_{89-94}\text{Ab}_{3-5}\text{Cs}_{2-6}$ ) relative to the rims ( $\text{Kfs}_{95-97}\text{Ab}_{2-5}\text{Cs}_{0-1}$ ). The core-rim boundary is complex and does not conform to the shape of the host crystal, which indicates that Ba depletion along the rim is a metasomatic overprint. Other primary phases include Ba-bearing biotite ( $\text{mg} \# = 0.40\text{--}0.53$ ;  $\text{Al}_2\text{O}_3 = 15.2\text{--}16.4$  wt. %;  $\text{TiO}_2 = 1.2\text{--}2.4$  wt. %;  $\text{F} = 0.5\text{--}1.4$  wt. %; up to 0.2 wt. % BaO) and apatite. Both these minerals are fractured, locally disaggregated and

replaced by late-stage phases (Figure GS-10-5e, -5f).

The order of crystallization of the late-stage paragenesis is albite  $\rightarrow$  calcite  $\rightarrow$  muscovite. The least modified varieties of pegmatite contain albite+calcite in fractures within the primary minerals and calcite+muscovite confined to interstitial spaces. The calcite-albite-muscovite aggregate locally grades into essentially monomineralic calcite, which is enriched in Sr (up to 1.7 wt. % SrO) and hosts minute inclusions of apatite, monazite and britholite. Magnetite and Mg-rich, Al-poor biotite ( $\text{mg} \# = 0.57\text{--}0.75$ ;  $\text{Al}_2\text{O}_3 = 10.8\text{--}14.9$  wt. %;  $\text{TiO}_2 = 0.3\text{--}1.0$  wt. %;  $\text{F} = 0.7\text{--}2.1$  wt. %) are believed to be part of the same mineral assemblage, but their temporal relations with respect to albite, calcite and muscovite are as yet uncertain.

Andradite veins crosscutting unit 2 are essentially monomineralic (Figure GS-10-2b); the total modal content of other constituents (titanite, biotite and calcite) does not exceed 5 vol. %. Compositionally, this andradite is different from that in units 1 and 2 in that it is enriched in Ti (7.2–7.8 wt. %  $\text{TiO}_2$ ), depleted in Al (1.5–1.6 wt. %  $\text{Al}_2\text{O}_3$ ) and contains detectable Mg and Y ( $\sim 0.4$  and 0.2 wt. % respective oxides).

## Geochemistry

Large fragments of the aegirine-nepheline syenite, biotite-vishnevite syenite and pegmatite ( $\sim 50$  g each) were cleaned, pulverized and analyzed for major- and trace-elements at Activation Laboratories Ltd. in Ancaster, Ontario. Conventional lithium-borate fusion and inductively coupled plasma-mass spectrometry techniques were used for all major- and trace-elements except  $\text{CO}_2$  (determined by coulometry), S (infrared analysis) and F (ion-selective-electrode analysis).

The feldspathoid syenites (units 1 and 2) have remarkably similar major- and trace-element geochemistry (Figure GS-10-6) in that both are potassic ( $\text{K}/\text{Na} = 1.5\text{--}2.0$ ) peralkaline rocks enriched in large-ion lithophile elements (particularly, Rb, Ba and Pb) and relatively depleted in high-field-strength elements (notably Ti, Nb and Ta). Unit 2 contains higher levels of K, S and  $\text{CO}_2$ , in agreement with the presence of vishnevite and a higher modal content of biotite in this rock. Most of the key trace-element ratios are close to primitive-mantle values ( $\text{Rb}/\text{K} = 0.003$ ;  $\text{Ba}/\text{K} = 0.03\text{--}0.04$ ;  $\text{Ga}/\text{Al} = 0.0002\text{--}0.0003$ ;  $\text{Y}/\text{Ho} = 27\text{--}28$ ;  $\text{Zr}/\text{Hf} = 40$ ;  $\text{Nb}/\text{Ta} = 23\text{--}24$ ), but both units show appreciable depletion in La relative to Ba ( $\text{Ba}/\text{La} = 15\text{--}33$ ), Sr relative to Ba ( $\text{Sr}/\text{Ba} = 0.5\text{--}0.6$ ) and enrichment in Th relative to Nb ( $\text{Th}/\text{Nb} = 0.6\text{--}1.4$ ) and Co relative to Ni and Cr ( $\text{Co}/\text{Ni} = 0.56\text{--}0.75$ ;  $\text{Co}/\text{Cr} = 0.22\text{--}0.33$ ). These characteristics indicate that the mantle source of the syenites has been geochemically modified (metasomatized) and that they represent derivative, rather than primary, melts.

The major- and trace-element geochemistry of the

<sup>4</sup> Kfs =  $\text{KAlSi}_3\text{O}_8$ ; Ab =  $\text{NaAlSi}_3\text{O}_8$ ; Cs =  $\text{BaAl}_2\text{Si}_2\text{O}_8$ ; Ne =  $\text{NaAlSiO}_4$ ; Ks =  $\text{KAlSiO}_4$ ; Qtz =  $\text{SiO}_2$  (all end-member components in mole per cent)

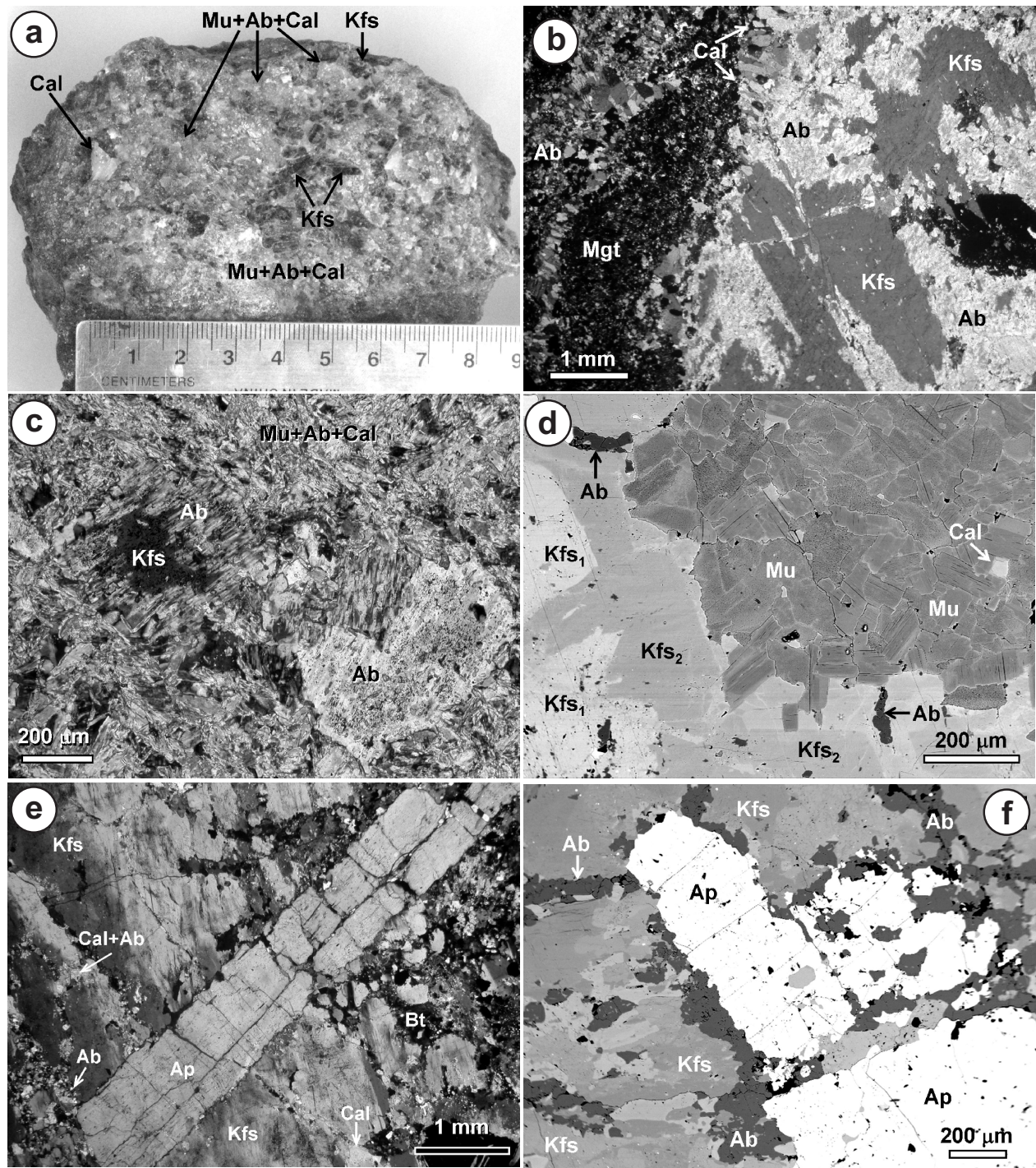


**Figure GS-10-5:** Textural characteristics of syenitic pegmatites from the Cinder Lake alkaline intrusive complex: **a)** hand specimen of typical pegmatite showing interrelations between potassium feldspar (Kfs) and late-stage minerals (Mu, muscovite; Ab, albite; Cal, calcite); **b)** replacement of potassium feldspar by albite (Ab, albite; Kfs, potassium feldspar; Mgt, magnetite), crossed-polarized light; **c)** albite pseudomorphs (Ab) after potassium feldspar (Kfs) from pegmatite almost entirely converted to a muscovite-albite-calcite aggregate, crossed-polarized light; **d)** zoning in potassium feldspar, comprising a Ba-enriched (Kfs<sub>1</sub>) and a Ba-depleted (Kfs<sub>2</sub>) rim, BSE image; **e)** mode of occurrence of primary apatite (Ap) and biotite (Bt) in a relatively fresh pegmatite, crossed-polarized light; **f)** disaggregated crystals of primary apatite (Ap) in pegmatite, BSE image.

## Normalized element abundances

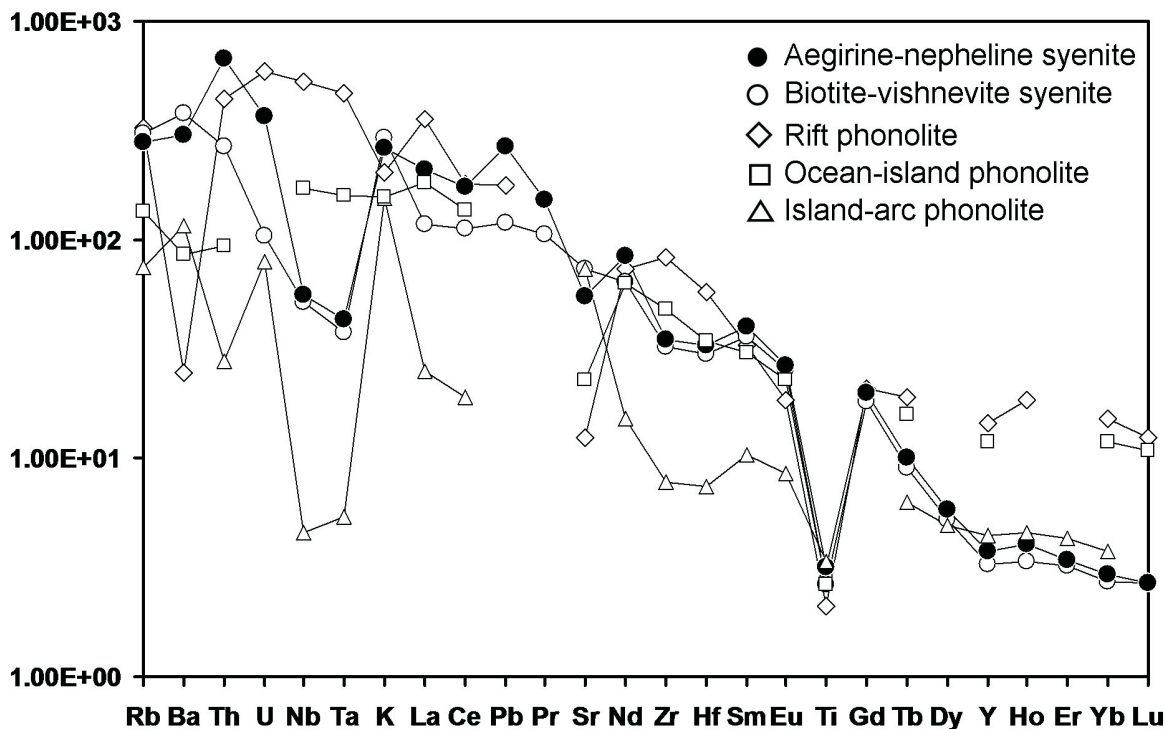


**Figure GS-10-6:** Abundances of selected trace elements in the Cinder Lake feldspathoid syenites normalized to the primitive mantle of McDonough and Sun (1995). The trace-element compositions of phonolites from a typical intracontinental rift (Kenya Rift: Hay et al., 1995), oceanic island (Kaula, Hawaii: Garcia et al., 1986) and arc environment (Lihir, Indonesia: Müller et al., 2001) are plotted for comparison.

pegmatite is highly variable due to large variations in the distribution and modal content of its six principal mineral constituents (potassium feldspar, apatite, biotite, albite, calcite and muscovite). In agreement with the petrographic data presented above, the most modified varieties of pegmatite contain relatively higher abundances of CO<sub>2</sub>, Ca, Sr, Ba, rare-earth elements (REE), Th and U, which are concentrated in calcite and its associated phosphate minerals.

### Petrogenetic implications

The combined field, petrographic and geochemical evidence indicates that the three types of alkaline rock presently identified at Cinder Lake are genetically related and represent discrete phases of intrusion. The order of emplacement is interpreted as aegirine-nepheline syenite → biotite-vishnevite syenite → syenitic pegmatite. The presence of relict diopside cores in aegirine phenocrysts from unit 1 and high Co/Ni and Co/Cr ratios in both types of feldspathoid syenite suggest the existence of a cumulate unit (magnetite-bearing clinopyroxenite?) at depth. The syenitic pegmatite may have crystallized from an evolved melt batch derived from unit 2 (Figure GS-10-2b). The pegmatite mineralogy has been heavily affected by metasomatism. The interstitial development of calcite-muscovite aggregate and the euhedral shape of

potassium feldspar crystals showing little albitization both indicate that, in addition to the feldspar, the pegmatite contained an unknown felsic mineral that was consumed during metasomatism. Although neither the nature nor the source of the metasomatic fluid can be ascertained at present, the abundance of Sr-rich calcite and associated REE-bearing phosphates in the late-stage paragenesis suggests a carbonatitic origin of the fluid. The abundant veining of unit 2 rocks by Ti-rich andradite in the vicinity of the pegmatite is also consistent with a carbonatitic overprint, as andradite is commonly developed at contacts between carbonatite bodies and diverse alkaline silicate rocks (e.g., Chakhmouradian et al., 2008). It is highly probable that carbonatite does occur at Cinder Lake but is not exposed due to the low chemical stability of calcite in a wet temperate climate.

Feldspathoid syenites and their extrusive analogues (phonolite and tephritic phonolite) occur in a number of tectonic settings but are most common in intracontinental rifts (e.g., Rhine graben and East African Rift; Wörner and Schmincke, 1984; Hay et al., 1995) and areas of oceanic intraplate magmatism (e.g., Hawaii and Fernando de Noronha; Garcia et al., 1986; Weaver, 1990). Published geochemical data show that, with rare exceptions, the feldspathoid phonolitic rocks that occur in these settings are sodic (averaging K/Na ~0.8 for both types)

and do not show depletion in trace high-field-strength elements (HFSE) relative to large-ion-lithophile elements. Rift-confined phonolite is commonly enriched in Nb+Ta and/or Zr+Hf, whereas its oceanic-island counterpart shows a relatively flat trace-element profile (Figure GS-10-5). Furthermore, the Zr/Hf ratio typically exceeds the primitive-mantle value in rift phonolite (averaging 55) and is consistently higher than 50 in oceanic-island phonolite. The latter is also characterized by superchondritic Nb/Ta values (averaging 33). The elevated Zr/Hf and Nb/Ta ratios reflect the highly fractionated nature of oceanic-island phonolite (e.g., Weaver, 1990). The Ba/La and Th/Nb ratios, believed to be a sensitive indicator of subduction input (e.g., Edwards et al., 1994; Patino et al., 2000), are close to the primitive-mantle values in both rift and oceanic-island phonolites. The average Ba/La and Th/Nb values for these rocks (5–9 and 0.13–0.18, respectively) are in sharp contrast with the high-Ba/La and high-Th/Nb signature of the Cinder Lake feldspathoid syenite. These geochemical differences are sufficient to rule out cratonic rifting or mantle-plume activity as the driving force behind the alkaline magmatism at Cinder Lake.

The geochemistry of the Cinder Lake rocks is most consistent with the HFSE-depleted, potassic, high Ba/La and high Th/Nb signature of arc magmas (e.g., Edwards et al., 1994; Müller et al., 2001). In common with the samples examined during this study, the few examples of island-arc and continental-margin phonolites described in the literature are typically potassic rocks with a primitive Zr/Hf ratio and strong enrichment in Ba relative to La and Th relative to Nb (Ba/La = 22–80 and Th/Nb = 0.25–1.7 for both tectonic settings; Müller et al., 2001; Bowerman et al., 2006). In the Cinder Lake area, the regional geological setting—in particular, the abundance of tonalite and granodiorite among the plutonic rocks and the predominance of subaerially deposited sedimentary rocks and calcalkaline volcanic rocks in the Oxford Lake Group (Corkery et al., 2000)—is more consistent with an active continental margin than an island-arc environment. This conjecture is in accord with the model of Lin et al. (2006), in which the 3.0 Ga North Caribou superterrane immediately south of the GLD “served as a nucleus onto which other terranes were accreted and both the northern and southern margins of the [superterrane] were Andean-type continental margins” (p. 763).

### **Economic considerations**

Feldspathoid syenite is a viable source of alumina, phosphate and metals for advanced technological applications. The high Al<sub>2</sub>O<sub>3</sub> content and chemical properties make nepheline a desirable low-cost substitute for bauxite, whereas apatite may be present in significant quantities in some silica-undersaturated alkaline rocks. For example, at the Khibiny alkaline complex in northwestern Russia, both apatite and nepheline are extracted from

mineralogically and texturally complex ores by stepwise flotation combined with magnetic separation to remove aegirine and magnetite. The Khibiny ore comprises from 38 to 55 wt. % nepheline and from 33 to 40 wt. % apatite, corresponding to a maximum grade of 19 wt. % Al<sub>2</sub>O<sub>3</sub> and 17 wt. % P<sub>2</sub>O<sub>5</sub> (Petrov, 2004). About 9 million tons of fertilizer-grade apatite and 900 000 tons of nepheline concentrate are produced at Khibiny annually. One ton of the concentrate yields approximately 130 kg of aluminum and 300 g of gallium, which are extracted from nepheline at half the cost of production from bauxite (Brylyakov et al., 1999). Importantly, the Khibiny deposit is the largest deposit of igneous apatite and nepheline in the world (~400 million tons of demonstrated and inferred reserves; Petrov, 2004), and it is unlikely that a deposit of that size would be overlooked in the course of detailed regional-scale mapping. Estimates of the size of the Cinder Lake intrusive body made during this study (on the order of 5 km<sup>2</sup>), its unfavourable geographic setting and the negligible content of apatite in all of the intrusive units imply that the alkaline silicate rocks investigated to date have no economic potential.

Carbonatite, the presence of which is inferred at Cinder Lake on the basis of indirect textural evidence, may be of significant interest to the mineral exploration sector as a host for REE, Ba and Sr mineralization. Of particular interest is its REE potential, as indicated by the abundance of REE-bearing minerals in association with calcite in metasomatized syenitic pegmatite and by the high levels of Y in vein andradite. Calcite carbonatite in collisional settings is particularly enriched in REE, in some cases reaching economic concentrations. For example, the Maoniuping syenite-carbonatite complex in southern China is the second largest REE deposit in the world, containing over 1.45 million tons of REE<sub>2</sub>O<sub>3</sub> in primary and enriched secondary ores ranging in grade from 2.7 to 13.6 wt. % REE<sub>2</sub>O<sub>3</sub> (Xu et al., 2004). The geological setting and size of the Maoniuping complex are similar to those of the Cinder Lake alkaline intrusive complex, but the former is coeval with the Himalayan orogeny and therefore much better exposed. Although it is almost certain that the putative Cinder Lake carbonatite will carry REE mineralization, locating both the putative carbonatite and its mineralized areas using conventional exploration techniques may prove prohibitively expensive.

Historically, exploration in the volcanic rocks between Cinder and Knee lakes has yielded drillhole intersects with anomalous Zn content. Between the late 1950s and early 1970s, Canico AEM and, subsequently, Barringer Magenta (Assessment File 91198, Manitoba Science, Technology, Energy and Mines, Winnipeg) conducted ground geophysics and diamond-drilling in the area and found chloritic and siliceous tuff intercalated with graphitic sediment in mafic volcanic rocks. Drill intersects up to several metres long were reported

to be associated with massive and brecciated pyrite and pyrrhotite with rare chalcopyrite and sphalerite, and assayed up to 0.38% Zn across the intersects. The massive sulphide zones, primarily developed in brecciated dacite, were interpreted as sulphide-rich exhalative zones and chlorite-garnet alteration. In 1994, Inco Exploration and Technical Services Inc. (Assessment File 94730) conducted a drill program that targeted the brecciated diabase and massive sulphide-rich zones. Drillcore from this program yielded assay results up to 0.86% Zn and 0.31% Cu over more than 20 m, and showed that the chloritic and garnetiferous volcanic breccia appears to be restricted to tholeiitic felsic to intermediate volcanic rocks of the Gods Lake (Hayes River) Group. Despite these results, no follow-up work has been done.

### Acknowledgments

This work was supported in part by the University of Manitoba (URGP grant to ARC) and the Natural Sciences and Engineering Research Council of Canada (Discovery grant to ARC and Undergraduate Student Research grant to RDK). The help of P. Yang (University of Manitoba) with electron-microprobe analysis is most gratefully acknowledged. The authors thank N. Brandson and D. Binne (MGS) for thorough logistical support. T. Corkery (MGS) is thanked for his help with sampling and for inspiring discussions at Cinder Lake.

### References

- Bowerman, M., Christianson, A., Creaser, R.A. and Luth, R.W. 2006: A petrological and geochemical study of the volcanic rocks of the Crowsnest Formation, southwestern Alberta, and of the Howell Creek suite, British Columbia; *Canadian Journal of Earth Sciences*, v. 43, p. 1621–1637.
- Brylyakov, Yu.E., Vasil'eva, N.Ya. and Petrovskii, A.A. 1999: Prospects of complex usage of apatite-nepheline ores; *Gornyi Zhurnal*, v. 9, p. 42–45 (in Russian).
- Chakhmouradian, A.R., Mumin, A.H., Demény, A. and Elliott, B. 2008: Postorogenic carbonatites at Eden Lake, Trans-Hudson Orogen (northern Manitoba, Canada): geological setting, mineralogy and geochemistry; *Lithos*, v. 103, p. 503–526.
- Corkery, M.T., Cameron, H.D.M., Lin, S., Skulski, T., Whalen, J.B. and Stern, R.A. 2000: Geological investigations in the Knee Lake Belt (parts of NTS 53L); *in* Report of Activities 2000, Manitoba Industry, Trade and Mines, Manitoba Geological Survey, p. 129–136.
- Corkery, M.T., Davis, D.W. and Lenton, P.G. 1992: Geochronological constraints on the development of the Cross Lake greenstone belt, northwest Superior Province, Manitoba; *Canadian Journal of Earth Sciences*, v. 29, p. 2171–2185.
- Davis, D.W., Amelin, Y., Nowell, G.M. and Parrish, R.R. 2005: Hf isotopes in zircon from the western Superior province, Canada: implications for Archean crustal development and evolution of the depleted mantle reservoir; *Precambrian Research*, v. 140, p. 132–156.
- Edwards, C.M.H., Menzies, M.A., Thirlwall, M.F., Morris, J.D., Leeman, W.P. and Harmon, R.S. 1994: The transition to potassic alkaline volcanism in island arcs: the Ringgit-Beser Complex, East Java, Indonesia; *Journal of Petrology*, v. 35, p. 1557–1595.
- Garcia, M.O., Frey, F.A. and Grooms, D.G. 1986: Petrology of volcanic rocks from Kaula Island, Hawaii: implications for the origin of Hawaiian phonolites; *Contributions to Mineralogy and Petrology*, v. 94, p. 461–471.
- Gilbert, H.P. 1985: Geology of the Knee Lake–Gods Lake area; Manitoba Energy and Mines, Geological Services, Geological Report GR83-1B, 76 p.
- Hay, D.E., Wendlandt, R.F. and Wendlandt, E.D. 1995: The origin of Kenya rift plateau-type flood phonolites: evidence from geochemical studies for fusion of lower crust modified by alkali basaltic magmatism; *Journal of Geophysical Research*, v. 100, p. 411–422.
- Heaman, L.M., Erdmer, P. and Owen, J.V. 2002: U-Pb geochronologic constraints on the crustal evolution of the Long Range Inlier, Newfoundland; *Canadian Journal of Earth Sciences*, v. 39, p. 845–865.
- Lenton, P.G. 1985: Granite-pegmatite investigations: Knee Lake–Magill Lake area; *in* Report of Field Activities 1985, Manitoba Energy and Mines, Geological Services, Mines Branch, p. 203–208.
- Lin, S., Davis, D.W., Rotenberg, E., Corkery, M.T. and Bailes, A.H. 2006: Geological evolution of the northwestern Superior Province: clues from geology, kinematics, and geochronology in the Gods Lake Narrows area, Oxford-Stull terrane, Manitoba; *Canadian Journal of Earth Sciences*, v. 43, p. 749–765.
- Lin, S. and Jiang, D. 2001: Using along-strike variation in strain and kinematics to define the movement direction of curved transpressional shear zones: an example from northwestern Superior Province, Manitoba; *Geology*, v. 29, p. 767–770.
- Ludwig, K.R. 2003: Isoplot 3.00: a geochronological toolkit for Microsoft Excel; Berkeley Geochronological Center, Special Publication No. 4, 70 p.
- McDonough, W.F. and Sun, S.-s. 1995: The composition of the Earth; *Chemical Geology*, v. 120, p. 223–253.
- Müller, D., Franz, L., Herzig, P.M. and Hunt, S. 2001: Potassic igneous rocks from the vicinity of epithermal gold mineralization, Lihir Island, Papua New Guinea; *Lithos*, v. 57, p. 163–186.
- Patino, L.C., Carr, M.J. and Feigenson, M.D. 2000: Local and regional variations in Central American arc lavas controlled by variations in subducted sediment input; *Contributions to Mineralogy and Petrology*, v. 138, p. 265–283.
- Percival, J.A., Sanborn-Barrie, M., Skulski, T., Stott, G.M., Helmstaedt, H. and White, D.J. 2006: Tectonic evolution of the western Superior Province from NATMAP and LITHO-PROBE studies; *Canadian Journal of Earth Sciences*, v. 43, p. 1085–1117.
- Petrov, S.V. 2004: Economic deposits associated with the alkaline and ultrabasic complexes of the Kola Peninsula; *in* Phoscorites and Carbonatites from Mantle to Mine: The Key Example of the Kola Alkaline Province (F. Wall and A.N. Zaitsev, ed.), The Mineralogical Society, Book Series, v. 10, p. 469–490.

- Schmidberger, S.S., Simonetti, A., Heaman, L.M., Creaser, R.A. and Whiteford, S. 2007: Lu-Hf, in-situ Sr and Pb isotope and trace element systematics for mantle eclogites from the Diavik diamond mine: evidence for Paleoproterozoic subduction beneath the Slave craton, Canada; *Earth and Planetary Science Letters*, v. 254, p. 55-68.
- Stacey, J.S. and Kramers, J.D. 1975: Approximation of terrestrial lead isotope evolution by a two-stage model; *Earth and Planetary Science Letters*, v. 26, p. 207-221.
- Stott, G.M. and Rayner, N., 2004: Discrimination of Archean domains in the Sachigo subprovince; *in* Summary of Field Work and Other Activities 2004, Ontario Geological Survey, Open File Report 6145, p. 10-1-10-8.
- Syme, E.C., Corkery, M.T., Bailes, A.H., Lin, S., Cameron, H.D.M. and Prouse, D. 1997: Geological investigations in the Knee Lake area, northwestern Superior Province; *in* Report of Field Activities 1997, Manitoba Energy and Mines, Geological Services, p. 37-46.
- Weaver, B.L. 1990: Geochemistry of highly-undersaturated ocean island basalt suites from the South Atlantic Ocean: Fernando de Noronha and Trindade islands; *Contributions to Mineralogy and Petrology*, v. 105, p. 502-515.
- Wörner, G. and Schmincke, H.-U. 1984: Mineralogical and chemical zonation of the Laacher See Tephra Sequence (East Eifel, W. Germany); *Journal of Petrology*, v. 25, p. 805-835.
- Xu, C., Zhang, H., Huang, Z., Liu, C., Qi, L., Li, W. and Guan, T. 2004: Genesis of the carbonatite-syenite complex and REE deposit at Maoniuping, Sichuan Province, China: evidence from Pb isotope geochemistry; *Geochemical Journal*, v. 38, p. 67-76.